Quantification of coarsening effect on response uncertainty in reservoir simulation

De Hoop, S.; Voskov, D. V.; Vossepoel, F. C.; Jung, A.

DOI
10.3997/2214-4609.201802223

Publication date
2018

Document Version
Final published version

Published in
16th European Conference on the Mathematics of Oil Recovery, ECMOR 2018

Th A1 05

Quantification Of Coarsening Effect On Response Uncertainty In Reservoir Simulation

S. de Hoop* (Delft University of Technology), D.V. Voskov (Delft University of Technology), F.C. Vossepoel (Delft University of Technology), A. Jung (Shell Global Solutions, The Netherlands)

Summary

In this study, an attempt is made to better understand the effect coarsening of the parameter space has on the uncertainty representation of the response. Firstly, an HF ensemble of channelized reservoir models is constructed using a Multi-Point Statistic (MPS) approach. Several levels of coarsening are generated using a flow-based upscaling algorithm. A water injection strategy is simulated for each scale of the hierarchical ensemble. Dynamic analysis is performed on a reduced representation of the response uncertainty obtained via Multidimensional Scaling (MDS). We introduce an Uncertainty Trajectory (UT), which quantifies the coarsening effect in terms of deviation from the HF ensemble response uncertainty. The UT also includes the temporal behavior of the response uncertainty of each ensemble scale. The mean integrated distance from the HF ensemble UT can be used as a measure of dissimilarity in the flow behavior of consecutive coarser ensembles scales. Reducing the number of HF flow simulations required for uncertainty quantification can be achieved via the proposed methodology and thereby greatly reducing the overall computational cost.

Introduction

Development of oil- and gas reservoirs are expensive operations which require a thorough understanding of the associated risks and uncertainties. Enhanced Oil Recovery methods as well as geothermal energy production amplify this demand even more. Uncertainties arise from the under-sampling of the subsurface which cause the estimation of geological parameters to be an underdetermined problem. A reservoir modeling workflow is typically adopted which captures the heterogeneity and complexity by representing the solution space with a large number of high-resolution reservoir models, denoted as a High Fidelity (HF) ensemble. The spread in flow response of the HF ensemble depicts the associated uncertainty in permeability and other fluid flow-related parameters. Common uncertainty quantification techniques such as Monte Carlo (MC) methods require a lot of evaluations of the state of the HF ensemble and can therefore become computationally expensive. A frequently used solution is coarsening the HF ensemble until satisfactory grid resolution is reached which allows for a consistently large ensemble to be evaluated for its flow response. It is however noted by several authors that certain biases arise when using coarser representations in the uncertainty quantification process (Lødøen et al., 2005). Other solutions exist which use proxy models in the form of streamline simulations in order to identify a subset of HF models on which subsequent uncertainty quantification is performed (Scheidt and Caers, 2009). The previously mentioned research has contributed significantly to the modern reservoir modeling workflow, in particular the use of a distance-based (metric space) approach which allows for reduced order modeling. This development has served as a major inspiration for this work.

In this study, an attempt is made to better understand the effect coarsening of the parameter space has on the uncertainty representation of the response. Firstly, a HF ensemble of channelized reservoir models is constructed using a Multi-Point Statistic (MPS) approach (Strebelle, 2002; Straubhaar et al., 2011). Several levels of coarsening are generated using a flow based upscaling algorithm (White et al., 1987; Holden and Nielsen, 2000). A water injection strategy is simulated for each scale of the hierarchical ensemble. Dynamic analysis is performed on a reduced representation of the response uncertainty obtained via Multidimensional Scaling (MDS) (Borg and Groenen, 2005). We introduce an Uncertainty Trajectory (UT), which quantifies the coarsening effect in terms of deviation from the HF ensemble response uncertainty. The UT also includes the temporal behavior of the response uncertainty of each ensemble scale. The mean integrated distance from the HF ensemble UT can be used as a measure of dissimilarity in the flow behavior of consecutive coarser ensembles scales. This is broadly explained in the following sections and illustrated with examples.

Due to the general nonlinear nature of the problems solved in the petroleum industry, models with seemingly different input parameters might have similar flow characteristics and therefore contribute in different extent to the overall ensemble uncertainty (see figure 1 for illustration). Such redundancies in the parameter space should be identified prior to expensive simulations and subsequent uncertainty quantification techniques (Insuasty et al., 2017). The uncertainty quantification methodology proposed in this work attempts to reduce the computational time by limiting the amount of HF ensemble evaluations and optimally use coarser information while converging to the same HF ensemble uncertainty quantification results. Finally, an endeavor is made to understand the relative quality of the presented uncertainty quantification methodology with respect to the most widely used MC analysis of the full HF ensemble.

Important ingredients of the analysis

In this section, we will describe all important definitions and methods used in our study.

Governing equations for forward simulation

The conservation of mass, in general form, is written as

$$F_c = \frac{\partial}{\partial t}\left(\phi \sum_p x_{cp}\rho_p S_p\right) + \nabla \cdot \sum_p x_{cp}\rho_p \mathbf{v}_p + \sum_p x_{cp}\rho_p q_p = 0, \quad c = 1,\ldots,n_c \tag{1}$$

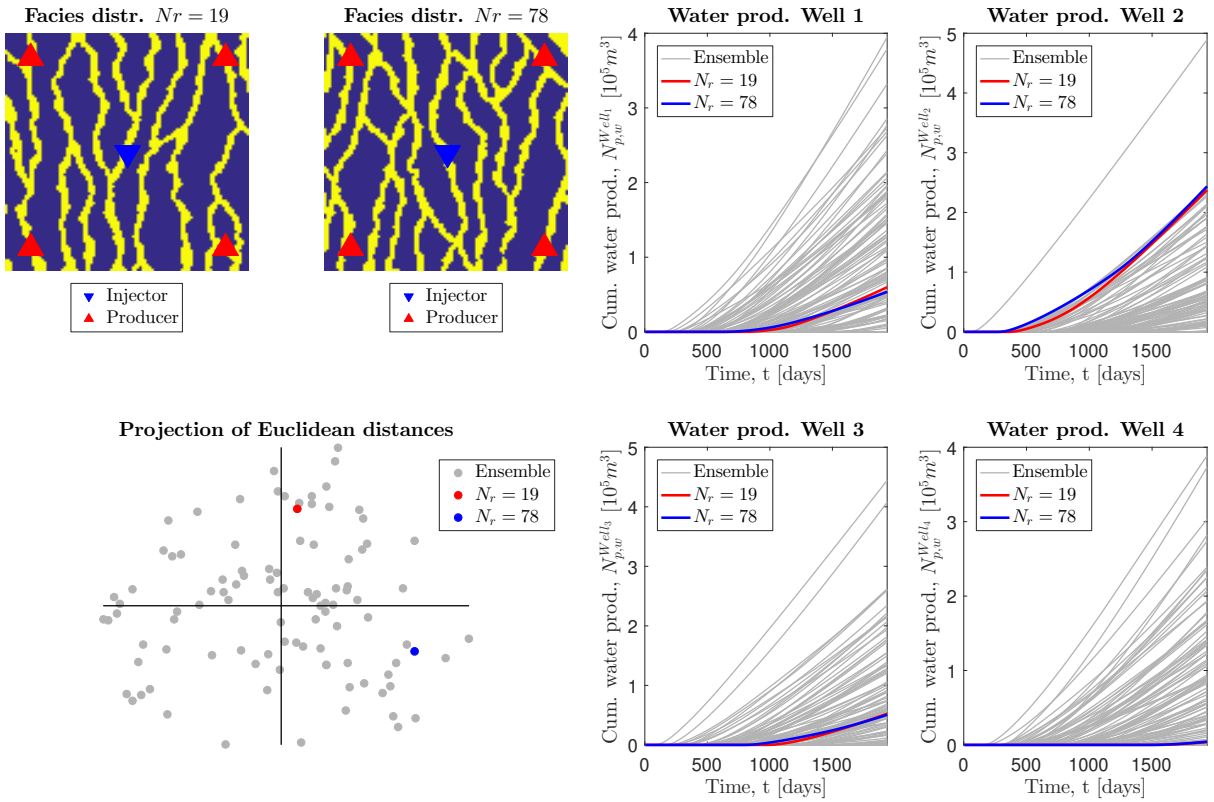

Figure 1 *Top left two images depict the facies, and hence permeability, distribution of two particular ensemble members. Bottom left shows the projected distances using MDS and a simple Euclidean distance between the permeability fields of each ensemble member. Right part of the figure displays the incredible similar flow characteristics of two seemingly different realizations. Modified from de Hoop (2017).*

where ϕ represents the porosity, x_{cp} is the molar mass fraction of component c in phase p, ρ_p is the density, S_p is the saturation, and q_p is the source term of the p-th phase respectively, $\mathbf{v}_p$ is the velocity of the p-th phase.

In this work, water injection into a dead oil reservoir is investigated and the governing equations can be simplified accordingly (Aziz and Settari, 1979)

$$\frac{\partial(\rho_p \phi S_p)}{\partial t} + \nabla \cdot (\rho_p \mathbf{v}_p) + \rho_p q_p = 0, \qquad p \in \{o, w\} \tag{2}$$

The Darcy velocity of the p-th phase is given by

$$\mathbf{v}_p = -\frac{k_{r,p}}{\mu_p} \mathbf{K} \nabla (P_p - \rho_p \mathbf{g}), \qquad p \in \{o, w\} \tag{3}$$

where $k_{r,p}$ is the relative permeability, μ_p is the viscosity and P_p is the pressure of the p-th phase respectively, $\mathbf{K}$ is the permeability tensor and $\mathbf{g}$ is the directional gravitational acceleration defined as $g\nabla z$. The governing equations are discretized and solved using the Automatic Differentiation General Purpose Research Simulator (ADGPRS) developed at Stanford University (Voskov, 2012; Zaydullin et al., 2014; Garipov et al., 2018).

Distance-based modeling and MDS

Distance-based methods and the use of a metric space in the reservoir modeling workflow have been investigated by several authors, see the works of Suzuki and Caers (2008), Caers et al. (2010), Scheidt

and Caers (2009), and Park and Caers (2007) for details. Distance-based modeling formulates the variability between the ensemble members in terms of a distance, which measures the dissimilarity between any two members $\mathbf{X}, \mathbf{Y} \in \mathbf{R}^n$ as a scalar value $d(\mathbf{X}, \mathbf{Y}) \in \mathbf{R}$. When this distance is chosen such that it qualifies as a metric, the resulting set of models and associated distances, $(\mathbf{M}, d)$, is referred to as a metric space. Reducing the dimensionality and complexity of the modeling task in a metric space can be easily achieved when a distance is chosen such that it has a large correlation with the purpose of the modeling effort (Caers et al., 2010). For example, a simple Euclidean distance between the permeability fields of each ensemble member, as shown in figure 1, incorrectly displays the dissimilarity between two ensemble members when their water production per well is concerned. If a distance is chosen which incorporates characteristics of the desired property, e.g. water production per well, much better results are obtained in terms of the predicted dissimilarity between each ensemble member.

One of the most common dimensionality reduction algorithms is MDS (Borg and Groenen, 2005). In MDS, the square symmetric distance matrix $\mathbf{D}$, obtained by taking the distances of a particular property between each ensemble member, is projected onto a Cartesian hyperplane (after double centering it around a origin) of dimension $N_{\mathtt{reduced}} = N_{\mathtt{m}} << N_{\mathtt{M}}$, where $N_{\mathtt{M}}$ is the size of the ensemble $\mathbf{M}$. More specifically, the required steps and corresponding equations are given in the Appendix, as also described in Borg and Groenen (2005) chapter 12.

The dimension $N_{\mathtt{m}}$ of the hyperplane required to accurately replicate the original $\mathbf{D}$, depends on the magnitude of the eigenvalues in equation 11 and typically $N_{\mathtt{m}}$ attains one or two when production data from wells are used in the computation of $\mathbf{D}$. More generally in geoscience problems $N_{\mathtt{m}}$ can range from one till six (Caers et al., 2010) dimension(s). Note that since both $\mathbf{D} = \mathbf{D}^T$ and $\mathbf{C}_M = \mathbf{C}_M^T$,

$$(-\frac{1}{2}\mathbf{C}_M\mathbf{D}^{(2)}\mathbf{C}_M)^T = -\frac{1}{2}\mathbf{C}_M^T(\mathbf{D}^{(2)})^T\mathbf{C}_M^T = -\frac{1}{2}\mathbf{C}_M\mathbf{D}^{(2)}\mathbf{C}_M \tag{4}$$

and therefore the eigenvalue decomposition in equation 11 is equal to the Singular Value Decomposition (SVD) when all eigenvalues are greater than zero, which is generally true for $\mathbf{D}$ in geoscience applications (Caers et al., 2010). This allows for efficient computation of $\mathbf{X}_m$ when very large ensemble sizes are concerned and $N_{\mathtt{m}} << N_{\mathtt{M}}$ such that a mere truncated SVD is required.

Figure 2 illustrates a synthetic flow response and projection via the outlined MDS procedure. Similar flow responses are projected in proximity on the $N_{\mathtt{m}} = 2$ dimensional plane after applying MDS. Therefore, they can be clustered accordingly and the full response can be accurately represented, in this simple synthetic example, by three representative realizations one from each cluster respectively.

Hierarchical ensemble

The two-dimensional "geologically-realistic" fluvial reservoir models used in this work, representing the HF ensembles, are generated using two different methods. Firstly, the Improved Parallel Multiple-point Algorithm Using a List Approach (IMPALA) (Straubhaar et al., 2011) implementation of MPS in JewelSuite™. Secondly, the semi-process based software Flumy (Grappe et al., 2016). The training image used for the MPS simulations is taken from Strebelle (2002). Examples of the resulting permeability fields of several HF ensemble members as well as the well configuration are shown in figure 3.

After establishing the HF ensemble, a hierarchical coarsening is achieved by using global upscaling, a flow-based upscaling algorithm (White et al., 1987; Holden and Nielsen, 2000). A similar technique was applied in Aliyev and Durlofsky (2017) for optimization with uncertainties. This upscaling algorithm finds the single-phase steady-state pressure solution and consecutively uses the fine-scale pressures and fluxes to obtain the coarse scale transmissibility values. Directly upscaling of transmissibility results in a better coarser representation of the fine-scale pressure field (Chen et al., 2003). Single-phase flow-based upscaling methods can yield a satisfactory representation of the fine-scale pressures, when simulations of water injection into oil reservoirs are concerned (Chen and Durlofsky, 2006). For a comprehensive explanation of the global upscaling technique, as well as several other methods, the reader is referred to Durlofsky (2005). Note that besides the transmissibility, also the coarse-scale well indices can be

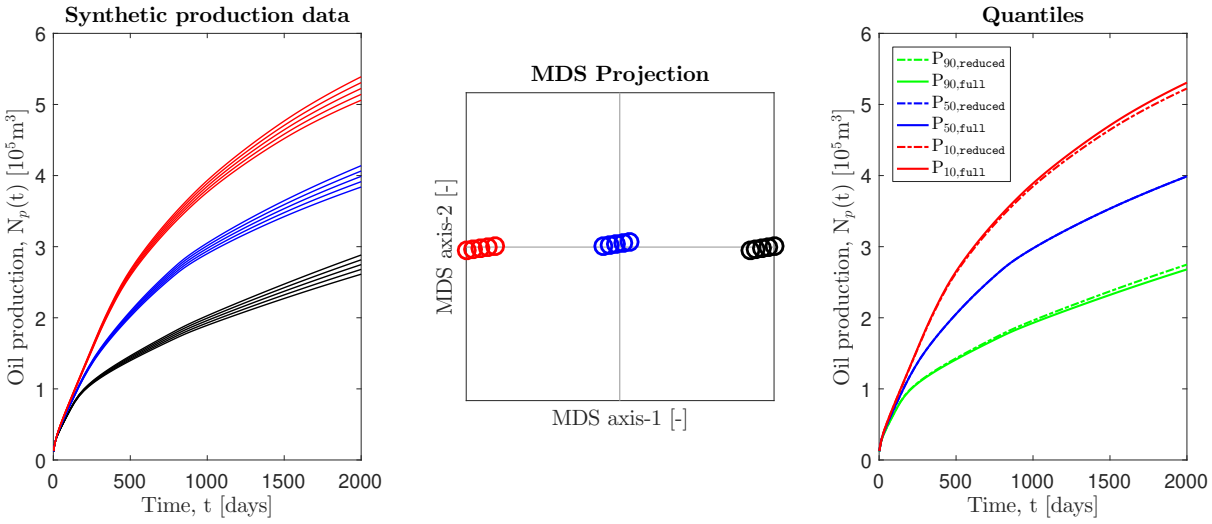

Figure 2 *Illustrating the resulting MDS projection on a synthetic production data set (left graph). Similar production curves will be projected in proximity on the reduced dimensional space (middle figure). Any type of clustering or grouping will identify similar responses and allow for a reduced set of models required for converging to the full ensemble uncertainty characteristics. This is illustrated in the right graph where only three realizations are used in the computation of the reduced quantiles.*

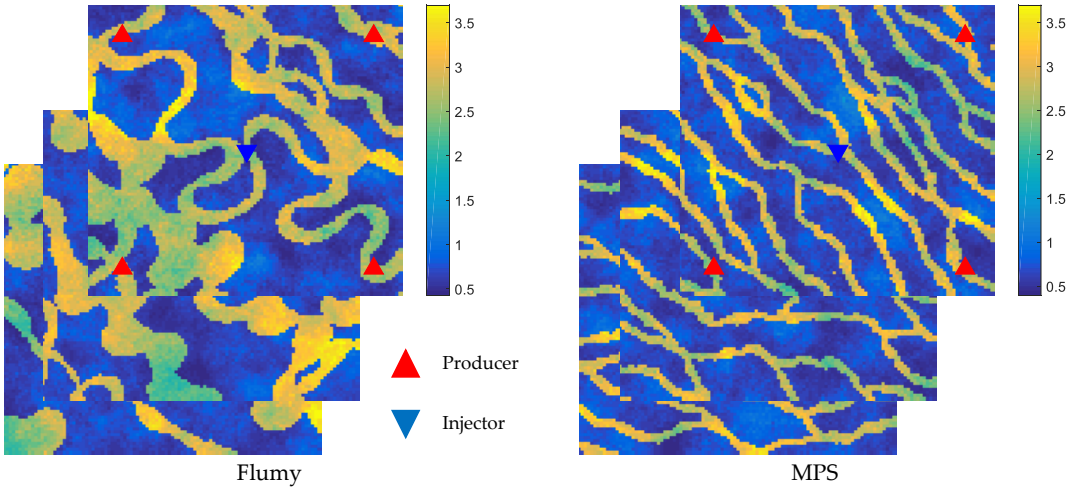

Figure 3 *Examples of the generated permeability fields (in* $\log_{10}$ *[mD]) using Flumy and MPS. The color bars indicate the magnitude of the permeability.*

computed in flow-based upscaling approach.

Hierarchy of Uncertainty Trajectories

The dynamic behavior of the response uncertainty is evident also in the MDS projections. The particular time interval of the response, used in computation of the square symmetric distance matrix **D**, has a large effect on the resulting MDS projection. This observation has led to the construction of an integrated MDS projection, where each projection is stacked subsequently in time in order to better describe the dynamic behavior of the uncertainty in time. Figure 4 displays the integration of MDS projections in time. Each particular projection $\mathbf{X}_i$, where $i = 1, 2, \ldots, N_t$ and N_t is the number of time-slices, is computed and positioned at its respective position in time.

In the integration process, allowing for any orthogonal transformation ensures a continuous representation of the uncertainty trajectory. Uncertainty trajectories are then build for the full hierarchical en-

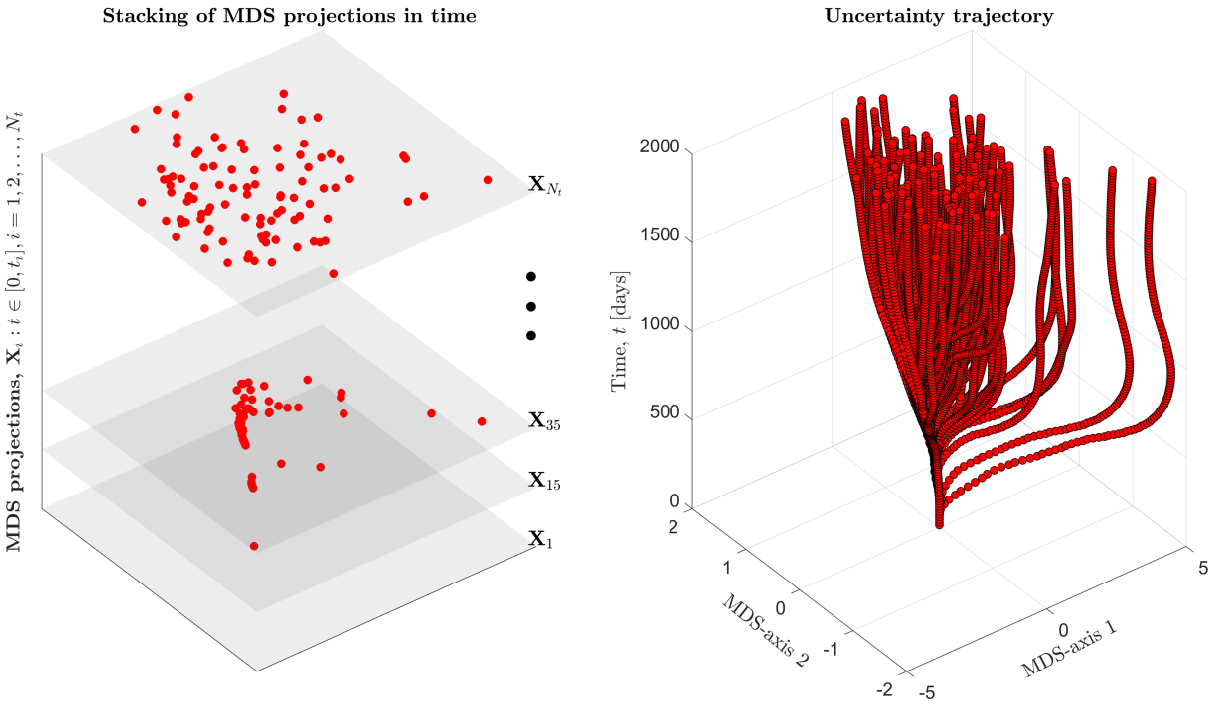

Figure 4 *The integration procedure of the MDS projections in time is depicted in the left image. The interval of the flow response of the ensemble, used in the computation of the square symmetric dissimilarity matrix* **D***, exhibits a strong effect on the resulting MDS projections. The right figure displays the continuous uncertainty trajectory of the full ensemble, showing the more stable behavior near the end of the simulation time.*

semble. This is depicted in figure 5 where uncertainty trajectories for each scale of the full hierarchy is shown, plotting merely two trajectories for illustration purposes. The coarsening effect is clearly visible in the uncertainty trajectories. Deviation from the HF trajectory, fairly monotonic as one would expect, generally shows an inward trend. This can be explained by a reduction of the variance in the flow response when coarsening, therefore reducing the relative distances between the coarser flow responses and resulting MDS projections. The flow responses used in this example can be found in the Appendix. The average integrated deviation from the finest uncertainty trajectory for all the properties used in figure 5 is shown in figure 6. The same trend is visible for each property, where property refers to the type of flow response used in computation of the square symmetric matrix of dissimilarities **D** in the MDS procedure.

Clustering of trajectories

Since clustering algorithms such as k-median and k-medoids are invariant to orthogonal transformations (Kaufman and Rousseeuw, 2009), Orthogonal Procrustes can be used to align each coarser trajectory with the HF trajectory, without changing the clustering results (Zhang, 2000). This allows for a measure of similarity in the temporal behavior of the uncertainty, in particular the similarity between the finest and respective coarser ensembles response uncertainty, and therefore attempts to describe the coarsening effect.

For completeness, the definition of Orthogonal Procrustes in terms of the singular value decomposition, as described by Zhang (2000) and originally Schönemann (1966), is

$$\mathbf{P} = (\mathbf{X}_i^{\mathtt{f}})^T \mathbf{X}_i^{\mathtt{c}} = \mathbf{U}\boldsymbol{\Sigma}\mathbf{V}^T \tag{5}$$

where $\mathbf{X}_i^{\mathtt{f}}$ is the MDS projection coordinate matrix of the i-th time-slice corresponding to the HF ensemble, while $\mathbf{X}_i^{\mathtt{c}}$ corresponds to the respective coarser ensembles in the established hierarchy. The columns of $\mathbf{U}$ and $\mathbf{V}$ contain the left- and right singular vectors whereas $\boldsymbol{\Sigma}$ corresponds to the matrix of

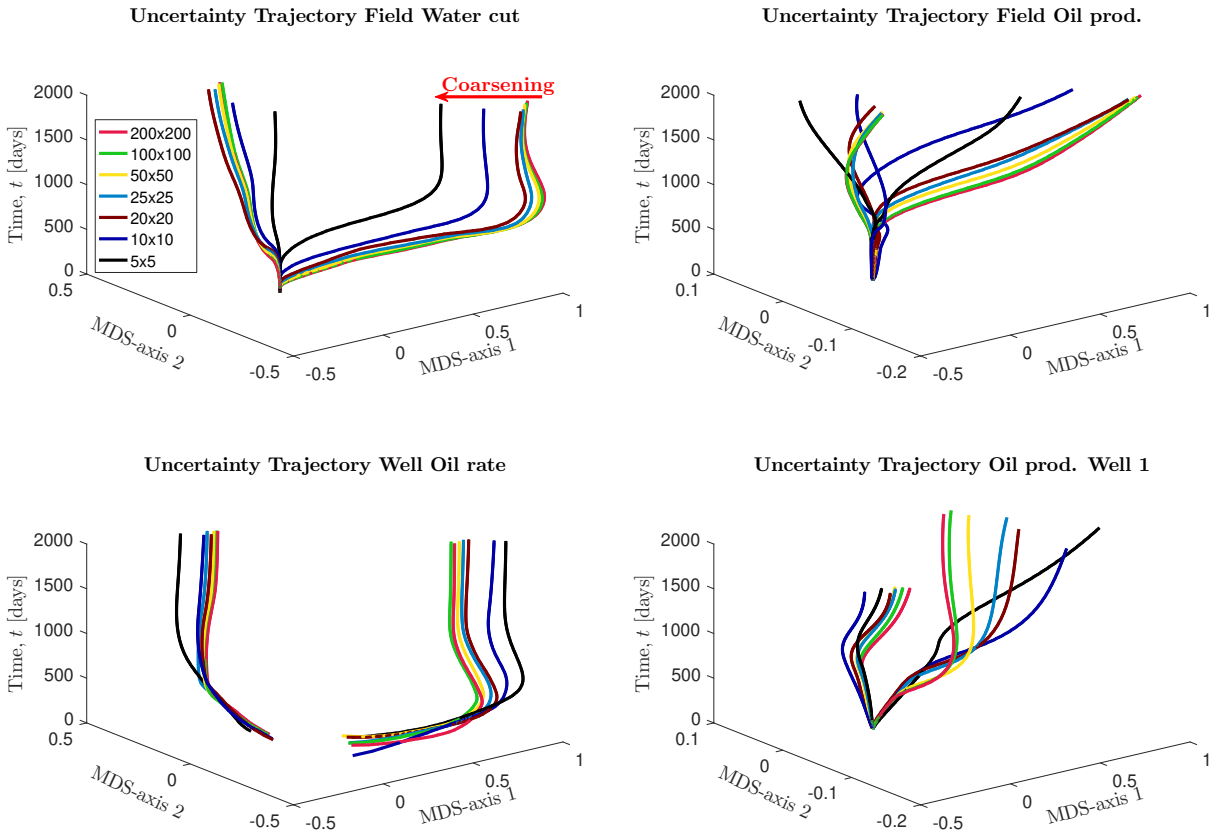

Figure 5 *Illustration of four different flow responses and their resulting uncertainty trajectories for the hierarchical ensemble. Note that only two trajectories of the full set are displayed. Modified from de Hoop (2017).*

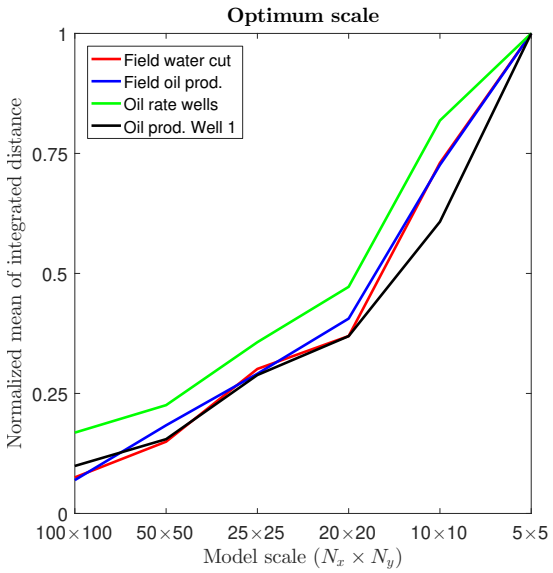

Figure 6 *Average integrated deviation from the HF uncertainty trajectory for the four properties used in figure 5.*

singular values. The orthogonal matrix describing the optimal rotation between the two MDS projection coordinate matrices is consequently obtained via

$$\mathbf{R}_{\mathtt{opt}} = \mathbf{V}\mathbf{U}^T \tag{6}$$

such that $||\mathbf{X}_i^{\mathtt{c}}\mathbf{R}_{\mathtt{opt}} - \mathbf{X}_i^{\mathtt{f}}||_F^2$ is minimized.

Deviation from the finest uncertainty trajectory after optimal rotation w.r.t the HF trajectory reveals the relative similarity in response uncertainty between each ensemble scale. When uncertainty trajectories of coarser models follow the HF trajectory "closely", any clustering or model selection procedure performed on the coarser ensemble response will result in a similar model selection on the HF ensemble scale. This is illustrated by figure 7 where certain ensemble scales display very strong similarity in the uncertainty trajectory, and therefore would result in the same model selection as one would obtain from directly clustering on the HF ensemble response. Note, however, that this is not true at every point in time. The trajectories of coarser models diverge for early to mid simulation times and ultimately, for particular levels of coarsening, converge back to the HF trajectory.

This suggests that the coarser information can be used as a distance for a model selection or ranking algorithm. The obtained subset of models is expected to represent the main characteristics of the full ensemble and therefore should provide the uncertainty quantification of the full HF ensemble. The idea of using proxy models or using coarser information for this purpose is not new, and the authors recognize earlier work from Scheidt et al. (2011), Scheidt and Caers (2009), Caers et al. (2010) and others. As illustrated by figure 7, caution should be taken when considering the time-interval over which the distances are computed as well as the magnitude of coarsening.

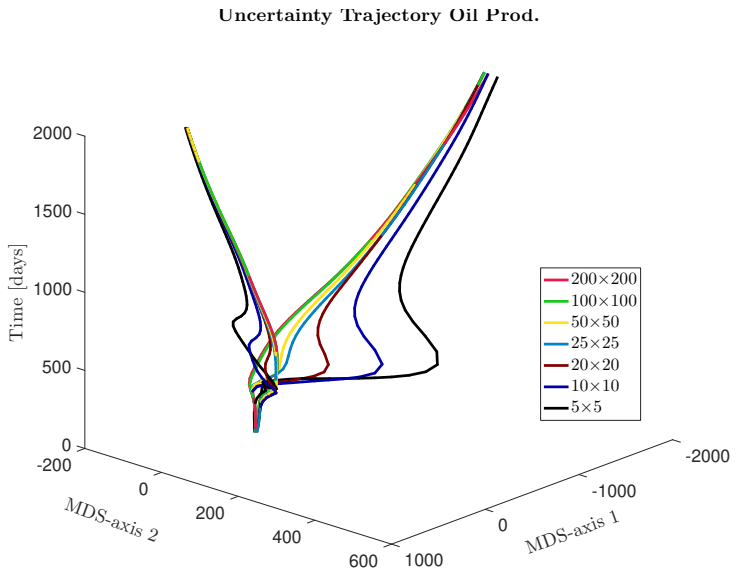

Figure 7 *Depicting two members of each ensemble scale uncertainty trajectory after allowing an optimal rotation via orthogonal procrustes at each time-slice. Clearly visible is the devation from the HF uncertainty trajectory for early to mid times while convergence is reached for almost all coarser trajectories near the end time.*

In this study, we establish a quantitative rule via comparison of the uncertainty trajectories for the relative quality of the coarse distance used in the MDS projection and subsequent model selection procedure. In principle the procedure requires knowledge of the full HF ensemble to precisely quantify the quality of clustering and subsequent uncertainty quantification with the subset of HF models. In practical applications this is generally not the case. The proposed quality check hinges on the correlations between the fine- and coarser scale flow responses as well as a direct comparison via the uncertainty trajectories of the subset of models. This seems to be sufficient for the models used in this work, but requires further validation.

The rate of convergence to the full ensemble uncertainty quantification for coarser ensembles can be used as an initial guess for the required number of clusters. Caution should be taken due to the variance reduction when coarsening, and a smaller number of realizations is required to describe the coarser uncertainty ranges (de Hoop, 2017). The convergence method for initializing the required number of clusters is adapted from Scheidt et al. (2009). In this method, the misfit between the full ensemble

(exhaustive set) and subset quantiles is given as follows (Scheidt et al., 2009)

$$\varepsilon_{N_K} = \frac{1}{3N_t}\sum_{i}^{N_t}\left(\left|P_{10}^{\texttt{full}}(t_i) - P_{10}^{\texttt{sub}}(t_i)\right| + \left|P_{50}^{\texttt{full}}(t_i) - P_{50}^{\texttt{sub}}(t_i)\right| + \left|P_{90}^{\texttt{full}}(t_i) - P_{90}^{\texttt{sub}}(t_i)\right|\right) \tag{7}$$

where N_k represents the number of clusters, i.e. size of the subset of HF models, N_t is the number of time-steps, and t_i represents the i-th time step.

The actual model-selection procedure is similar to that as presented in Scheidt et al. (2009, 2011) and a figure illustrating this can be found in the Appendix. Caution is advised, when considering the time interval over which the distances are computed. This is illustrated in the previous section by the use of uncertainty trajectories and the erroneous temporal behavior that can occur in coarser representations. Note that when constructing the quantiles for the subset of flow responses, their probability is being weighted by the size of the cluster which they represent.

Results

A larger ensemble consisting of 600 realizations with permeability fields as shown figure 3 is generated, hierarchical upscaled and finally subjected to a water-flooding experiment using the well configuration as shown in this same figure. For the flow simulations, a constant flow rate for the injection wells of 500[m^3/day] is used, the production wells are held at a constant bottomhole pressure of 100[bar], whereas the original reservoir pressure is set to 200[bar]. The following field production data was obtained, displayed in figure 8. The full ensemble response is plotted using a light gray color while the quantiles, which are often used to describe uncertainty ranges, are displayed using red, green and blue colors. It is evident that the uncertainty in permeability distribution results in a large spread in the response uncertainty and therefore would serve as an ideal test case for the above outlined methodology.

Uncertainty trajectories are computed for each ensemble in the hierarchy, as described in the previous section, and figure 9 shows deviations from the HF ensemble when coarsening. Similar trends in deviation are seen compared to the smaller ensemble size used in the previous section (which has a much smaller variability or spread in production data).

Deciding the required number of clusters for accurately representing the full ensemble uncertainty quantification requires knowledge on the variance of the flow response of the full ensemble. A convergence test is shown in figure 10, using the methodology adopted from Scheidt et al. (2009). The initial guess for the required number of clusters can be based on such a test for the particular coarser ensemble scale chosen for computation of MDS projection. The red line in figure 10 shows the misfit between the coarse-scale subset and the full ensemble quantiles, as defined in equation 7. The blue line represents the misfit between the full HF ensemble and the HF subset. Convergence of the red line is reached faster for higher levels of coarsening. This is expected since the variance is greatly reduced in the coarser ensemble scales and therefore less clusters are required to represent the characteristics of the full ensemble. Convergence of the blue line is much smoother and well behaved for moderate to low levels of coarsening. This is also expected since the flow responses for these spatial scales more accurately mimic the HF scale and therefore the distance used for computation of **D** and subsequent MDS procedure can be considered of higher quality. Figure 11 displays three different comparisons of quantiles using different coarser ensemble scales as well as number of clusters in computation of the subset quantiles.

As previously mentioned, the full HF ensemble response is inherently unknown in real life cases, therefore we can never with 100% certainty examine the quality of the model selection procedure and resulting subset statistics. However, when the uncertainty trajectory of coarser ensembles closely follow the HF trajectory, a similar model selection is obtained on both ensemble scales. Comparison is made in figure 12 between the full and subset statistics. The quality of the coarse distance is calculated using a linear correlation in breakthrough times between the HF and coarser scales respectively. This is done both for the full ensemble and the subset of models. A relative large decrease in correlation is paired with a relative large increase in the mean integrated distance from the HF uncertainty trajectory. This result

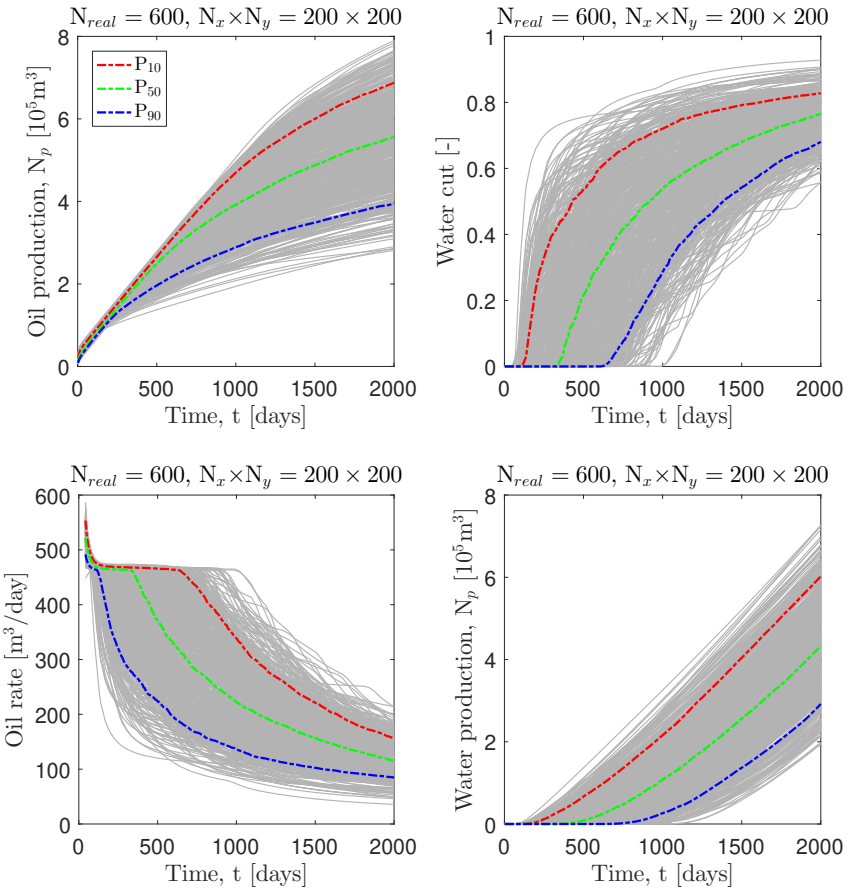

Figure 8 *Field production data obtained from forward simulations on the HF ensemble, consisting of 600 ensemble members.*

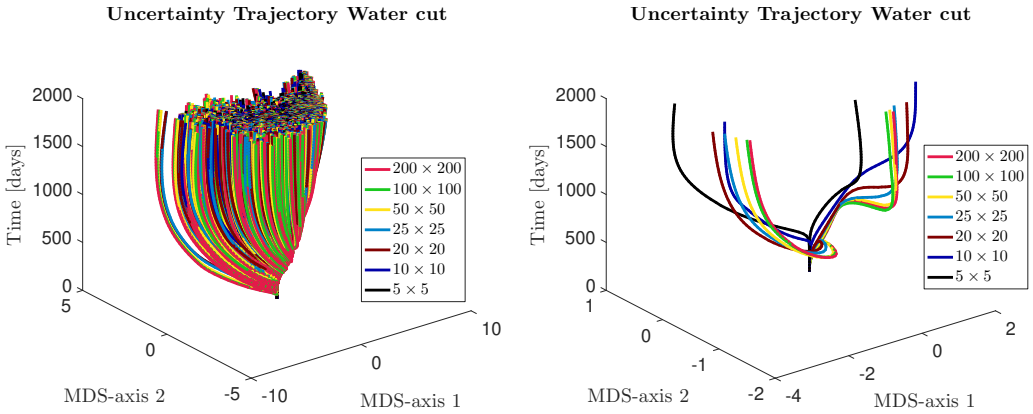

Figure 9 *Uncertainty trajectory for the full hierarchical ensemble. All the 600 curves for each scale are shown in the left plot. This is used in the computation of the mean integrated distance from the HF trajectory. The right figure shows for clarification purposes, the deviation from the HF ensemble when coarsening, similar to that in the example.*

is obtained for both the full ensemble and the subset of models, indicating that for this particular case, the selected subset of HF models accurately describes the overall variability of the full HF ensemble.

Considering that only the full coarse ensemble and the subset of coarse and HF flow responses are know, the following approach is suggested. When a strong correlation exists (close to one) between the subset of coarse and HF scale flow responses, the subset of coarse flow responses accurately predicts the full coarse variance over time, and the deviation (mean integrated distance) from the HF-subset uncertainty

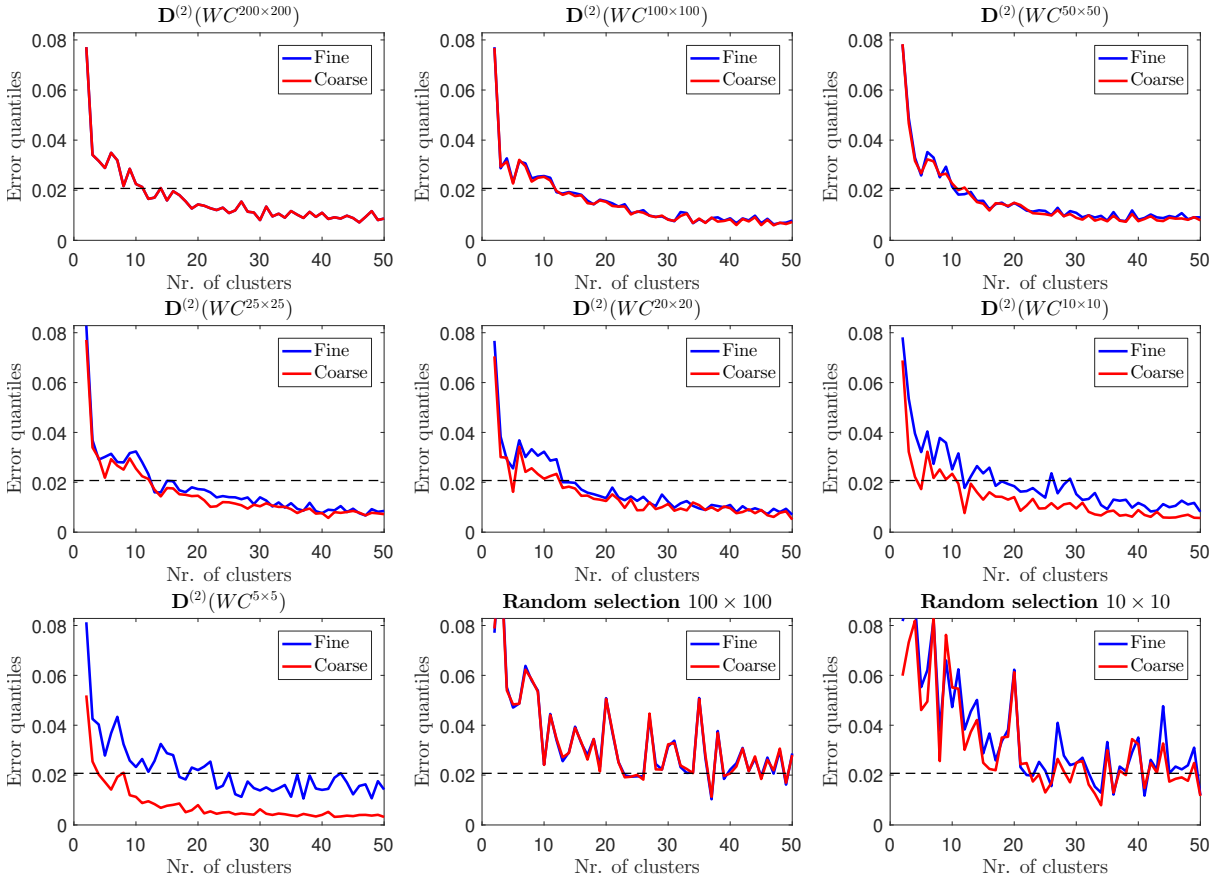

Figure 10 *Convergence rate between the full ensemble and subset quantiles. The red curve represents the misfit between the coarse subset and coarse full ensemble quantiles for that particular scale. The blue curve represents the misfit between the HF subset and the full HF ensemble, where the subset is obtained via the coarse distance in flow response for that particular scale. The flow response chosen to compute the coarse distance is field water cut. A more stable convergence rate, when increasing the number of clusters, is obtained if large correlation exists between fine- and coarse-scale flow response. This is logical since the distance used in the computation of the MDS projection is of high quality, and therefore represents the characteristics of the HF ensemble more accurately. As a comparison, the middle and right subfigure on the bottom row display convergence rate for random picking of model representatives.*

trajectory is small, a good model selection is obtained and full HF ensemble statistics can be deduced accurately from this subset of responses. The uncertainty trajectory also serves as a check to verify if the time interval on which the model selection is done, accurately represents the HF projection. The required number of clusters is not well defined and depends on the desired accuracy and size of the full HF ensemble. The difference in variance between the full coarse-scale flow response and the selected coarse-scale subset of models should be a fairly good indicator of the ultimate number of clusters required.

Conclusions

Understanding the temporal behavior of the response uncertainty across various ensemble scales is useful when considering utilizing the coarser flow responses to obtain a subset of HF models which aim to accurately represent the full HF ensemble. The proposed uncertainty trajectory attempts to do exactly that. Combining the uncertainty trajectories with a correlation and variance check, provides valuable information on the quality of the model selection and prediction of the full HF ensemble statistics. Finally, combining the convergence rate as a function of number of clusters on the coarse scale, additional information on the number of clusters required to accurately represent the full ensemble statistics is obtained.

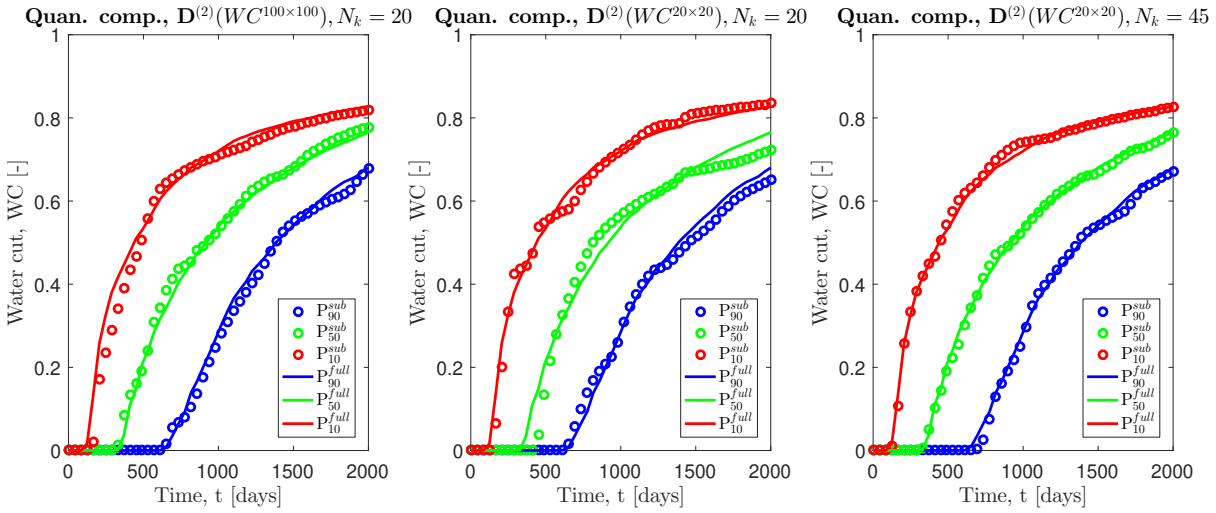

Figure 11 *Comparison between full HF ensemble and HF subset quantiles, for different number of clusters and coarse scale distances.*

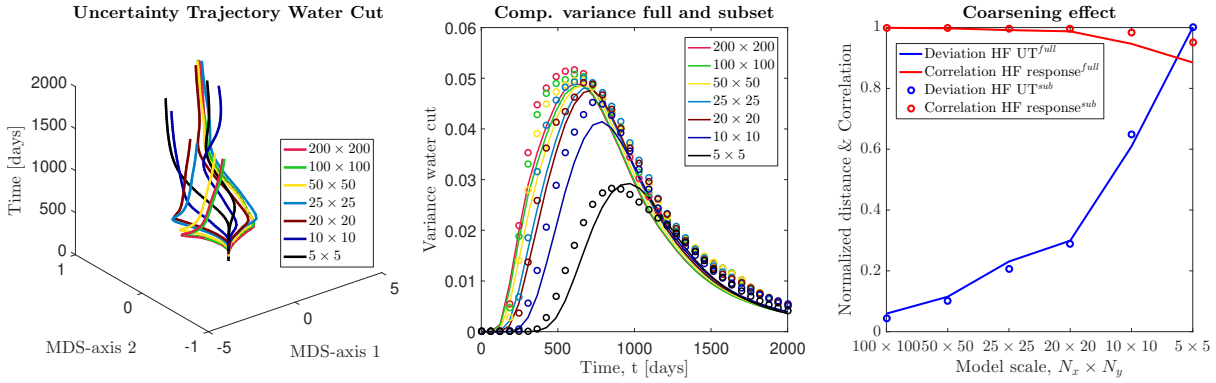

Figure 12 *General comparison of the full and subset statistics. Left image depicts the subset uncertainty trajectories for each ensemble scale. The middle figures displays the variance of the full ensemble (continuous line) and subset of models (circles) for each scale. Right image displays the correlation and deviation from the HF scale for both the full ensemble (continuous line) and subset of models (circles). Similar trends can be observed for both.*

The reservoir models considered in this work are what is called "geologically young" (Galloway and Hobday, 2012). This term holds for reservoirs which haven't experienced a lot of diagenesis and burial related transformation that affect the heterogeneity of the reservoir. This additional form of heterogeneity, typically expressed as fractured networks and pore-space related features, should be included in further work. Including these features will increase the variability in flow response and therefore increase the difficulty of representing the full HF ensemble statistics with a subset of HF models.

The dimensionality reduction method used in this work is a fairly simple one and newer and possibly better algorithms exists. The same holds for the clustering algorithm, see e.g. affinity propagation (Frey and Dueck, 2007) as an alternative for clustering, and kernel methods or Hessian LLE (Donoho and Grimes, 2003) for the dimensionality reduction (projection of the square symmetric distance matrix **D**). These newer methods might increase the linear separation and hence increase the quality of the clustering, which hinges on linear distances between each data point (e.g. for k-medoids). Reducing the number of HF flow simulations required for uncertainty quantification can be achieved via the proposed methodology and thereby greatly reducing the overall computational cost.

Acknowledgements

The authors would like to thank Stanford University for using the ADGPRS software for running the flow simulations, Baker Hughes, a GE company (BHGE) for using JewelSuite™ for the MPS simulations, MINES ParisTech / ARMINES for using Flumy for the semi-process based simulations.

Appendix

Steps and equations required for obtaining the MDS projections, as described in Borg and Groenen (2005) chapter 12:

1. Compute the square symmetric matrix of squared dissimilarities $\mathbf{D}^{(2)}$, where $^{(2)}$ denotes the square of the individual elements of the matrix $\mathbf{D}$.
2. Compute the centering matrix $\mathbf{C}_M$, defined as
$$\mathbf{C}_M = \mathbf{I}_M - \frac{1}{M}\mathbf{1}\mathbf{1}^T \tag{8}$$
where $\mathbf{I}_M$ is the identity matrix of dimensions $N_\mathtt{M} \times N_\mathtt{M}$, $\mathbf{1}$ is a vector of all ones with dimension $N_\mathtt{M} \times 1$ and $\cdot^T$ denotes the transpose.
3. Double center the matrix $\mathbf{D}^{(2)}$, using the computed centering matrix, such that
$$\mathbf{B} = -\frac{1}{2}\mathbf{C}_M\mathbf{D}^{(2)}\mathbf{C}_M \tag{9}$$
4. Compute an eigenvalue decomposition of $\mathbf{B}$, such that
$$\mathbf{B} = \mathbf{Q}\mathbf{\Lambda}\mathbf{Q}^T \tag{10}$$
5. Ordering the eigenvalues as $\lambda_1 \geq \lambda_2 \geq \ldots \geq \lambda_m \geq 0 \geq \lambda_{m+1} \geq \ldots \geq \lambda_M$ and the eigenvectors accordingly, such that $\mathbf{\Lambda}_m$ and $\mathbf{Q}_m$ contain the first m non-zero eigenvalues and associated eigenvectors respectively, the new coordinates of the projection onto the $N_\mathtt{m} = N_\mathtt{reduced}$ dimensional hyperplane, can be expressed as
$$\mathbf{X}_m = \mathbf{Q}_m\mathbf{\Lambda}_m^{1/2} \tag{11}$$
where the square root of a diagonal matrix is simply the square root of the individual diagonal entries.

The flow responses used for the computation of $\mathbf{D}$ and following uncertainty trajectories in figure 5 are displayed in the following figure.

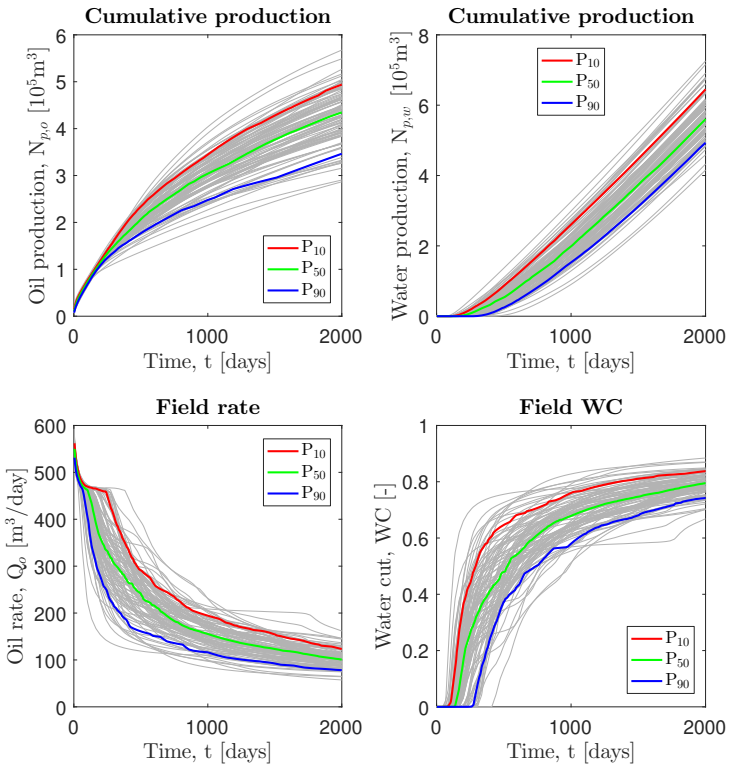

Figure 13 *Example of flow responses of the HF ensemble, used for the example in the theory and methods section.*

The following figure is taken from (de Hoop, 2017) and illustrated the model selection procedure.

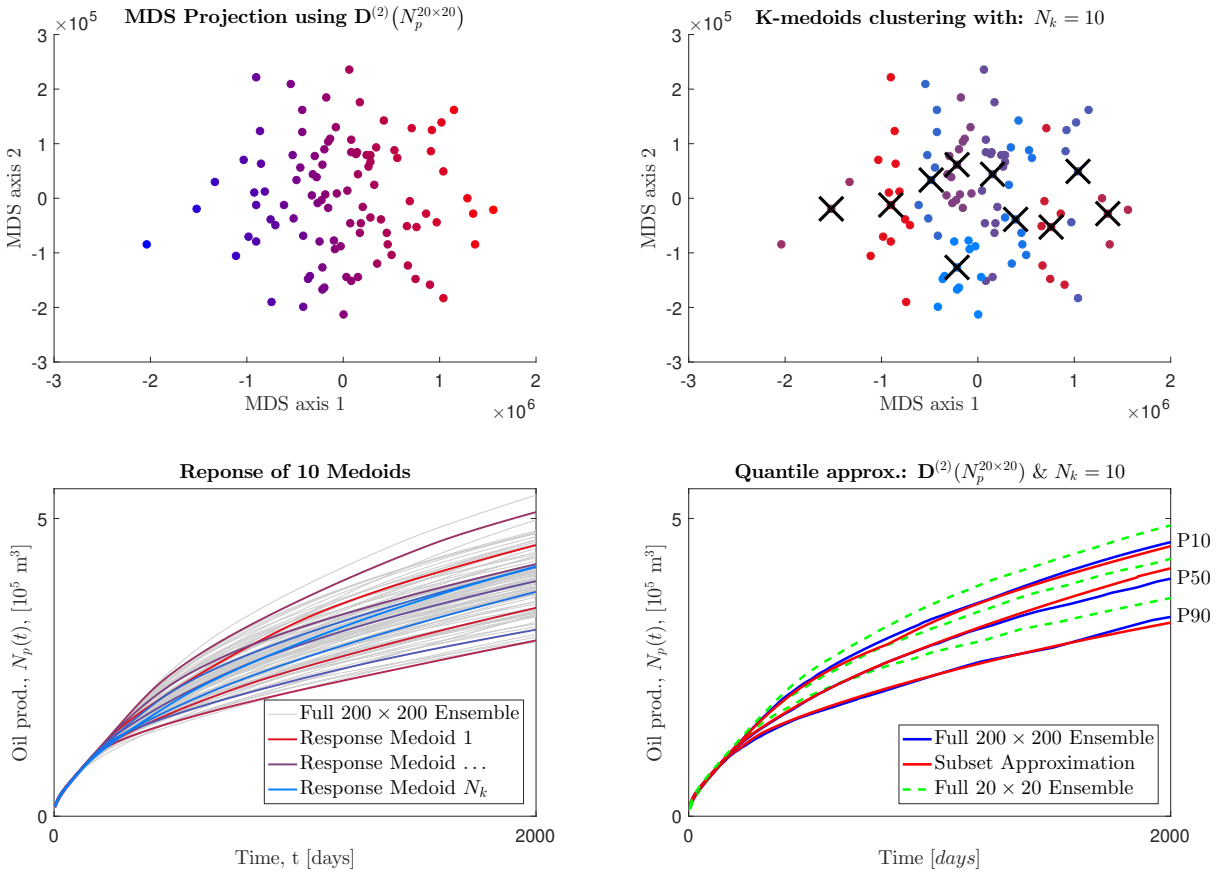

Figure 14 *Displaying the model selection procedure. Take distance for the particular property and coarser ensemble scale in the top left figure. The color represents the end cumulative production and displays a clear linear separation. Then, computation of the k-medoids clustering in the top right figure. Simulate subset of HF representatives forward in time in the bottom left graph. Computation of the subset statistics and compare with full ensemble in the bottom right. Modified from (de Hoop, 2017).*

References

Aliyev, E. and Durlofsky, L.J. [2017] Multilevel field development optimization under uncertainty using a sequence of upscaled models. *Mathematical Geosciences*, **49**(3), 307–339.

Aziz, K. and Settari, A. [1979] *Petroleum reservoir simulation*. Chapman & Hall.

Borg, I. and Groenen, P.J. [2005] *Modern multidimensional scaling: Theory and applications*. Springer Science & Business Media.

Caers, J., Park, K. and Scheidt, C. [2010] Modeling uncertainty of complex earth systems in metric space. In: *Handbook of Geomathematics*, Springer, 865–889.

Chen, Y. and Durlofsky, L.J. [2006] Adaptive local–global upscaling for general flow scenarios in heterogeneous formations. *Transport in porous Media*, **62**(2), 157–185.

Chen, Y., Durlofsky, L.J., Gerritsen, M. and Wen, X.H. [2003] A coupled local–global upscaling approach for simulating flow in highly heterogeneous formations. *Advances in Water Resources*, **26**(10), 1041–1060.

Donoho, D.L. and Grimes, C. [2003] Hessian eigenmaps: Locally linear embedding techniques for high-dimensional data. *Proceedings of the National Academy of Sciences*, **100**(10), 5591–5596.

Durlofsky, L.J. [2005] Upscaling and gridding of fine scale geological models for flow simulation. In: *8th International Forum on Reservoir Simulation Iles Borromees, Stresa, Italy*, 2024.

Frey, B.J. and Dueck, D. [2007] Clustering by passing messages between data points. *science*, **315**(5814), 972–976.

Galloway, W.E. and Hobday, D.K. [2012] *Terrigenous clastic depositional systems: Applications to fossil fuel and groundwater resources*. Springer Science & Business Media.

Garipov, T., Tomin, P., Rin, R., Voskov, D. and Tchelepi, H. [2018] Unified Thermo-Compositional-Mechanical Framework for Reservoir Simulation. *Computational Geosciences*.

Grappe, B., Cojan, I., Ors, F. and Rivoirard, J. [2016] Dynamic Modelling of Meandering Fluvial Systems at the Reservoir Scale, FLUMY Software. In: *Second Conference on Forward Modelling of Sedimentary Systems*.

Holden, L. and Nielsen, B.F. [2000] Global upscaling of permeability in heterogeneous reservoirs; the output least squares (ols) method. *Transport in Porous Media*, **40**(2), 115–143.

de Hoop, S. [2017] *Determination of Relevant Spatial Scale in Reservoir Simulation, MSc. Thesis*. Delft University of Technology.

Insuasty, E., Van den Hof, P.M., Weiland, S. and Jansen, J.D. [2017] Flow-based dissimilarity measures for reservoir models: a spatial-temporal tensor approach. *Computational Geosciences*, **21**(4), 645–663.

Kaufman, L. and Rousseeuw, P.J. [2009] *Finding groups in data: an introduction to cluster analysis*, 344. John Wiley & Sons.

Lødøen, O.P., Omre, H., Durlofsky, L.J. and Chen, Y. [2005] Assessment of uncertainty in reservoir production forecasts using upscaled flow models. In: *Geostatistics Banff 2004*, Springer, 713–722.

Park, K. and Caers, J. [2007] History matching in low-dimensional connectivity-vector space. In: *EAGE Conference on Petroleum Geostatistics*.

Scheidt, C. and Caers, J. [2009] Representing spatial uncertainty using distances and kernels. *Mathematical Geosciences*, **41**(4), 397.

Scheidt, C., Caers, J., Chen, Y. and Durlofsky, L.J. [2011] A multi-resolution workflow to generate high-resolution models constrained to dynamic data. *Computational Geosciences*, **15**(3), 545–563.

Scheidt, C., Caers, J. et al. [2009] Uncertainty Quantification in Reservoir Performance Using Distances and Kernel Methods–Application to a West Africa Deepwater Turbidite Reservoir. *SPE Journal*, **14**(04), 680–692.

Schönemann, P.H. [1966] A generalized solution of the orthogonal procrustes problem. *Psychometrika*, **31**(1), 1–10.

Straubhaar, J., Renard, P., Mariethoz, G., Froidevaux, R. and Besson, O. [2011] An improved parallel multiple-point algorithm using a list approach. *Mathematical Geosciences*, **43**(3), 305–328.

Strebelle, S. [2002] Conditional simulation of complex geological structures using multiple-point statistics. *Mathematical geology*, **34**(1), 1–21.

Suzuki, S. and Caers, J. [2008] A distance-based prior model parameterization for constraining solutions of spatial inverse problems. *Mathematical geosciences*, **40**(4), 445–469.

Voskov, D. [2012] An Extended Natural Variable Formulation for Compositional Simulation Based on Tie-Line Parameterization. *Transport in Porous Media*, **92**(3), 541–557. Cited By 2.

White, C., Horne, R. et al. [1987] Computing absolute transmissibility in the presence of fine-scale heterogeneity. In: *SPE symposium on reservoir simulation*. Society of Petroleum Engineers.

Zaydullin, R., Voskov, D., James, S., Henley, H. and Lucia, A. [2014] Fully compositional and thermal reservoir simulation. *Computers & Chemical Engineering*, **63**, 51–65.

Zhang, Z. [2000] A flexible new technique for camera calibration. *IEEE Transactions on pattern analysis and machine intelligence*, **22**(11), 1330–1334.